UNIVERSITY
OF WEST BOHEMIA

Applied and Computational Mechanics 2 (2008) 357–368

Applied and Computational Mechanics

Dynamical properties of the growing continuum using multiple-scale method

J. Rosenberg[a,*], L. Hynčík[a]

[a] Faculty of Applied Sciences, University of West Bohemia in Pilsen, Univerzitní 22, 306 14 Plzeň, Czech Republic

Received 26 August 2008; received in revised form 20 October 2008

Abstract

The theory of growth and remodeling is applied to the 1D continuum. This can be mentioned e.g. as a model of the muscle fibre or piezo-electric stack. Hyperelastic material described by free energy potential suggested by Fung is used whereas the change of stiffness is taken into account. Corresponding equations define the dynamical system with two degrees of freedom. Its stability and the properties of bifurcations are studied using multiple-scale method. There are shown the conditions under which the degenerated Hopf's bifurcation is occuring.

Keywords: muscle fibre, growth, multiple scale method, Hopf's bifurcation

1. Introduction

This contribution joins the previous papers of the authors — e.g. [3] — dealing with the application of the growth and remodelling theory (GRT) according to DiCarlo et al. — e.g. [1] — on the muscle fibre modelling. This approach allows to take into account also the change of the stiffness of the muscle fibre during the time. This effect was experimentally approved and modeled — see e.g. [2] or [5]. The same approach can be used to model the time evolution of the piezo-electric stack [6] but this case will not be discussed here. In both cases the final formulation has the form of the dynamical system with two degrees of freedom. The numerical experiments have shown the interesting behavior of this system, e.g the existence of some bifurcations. This contribution is devoted to the analysis of these properties using the multi-scale method (MSM). This method is the kind of the perturbation method and in general allows to decrease the number of degrees of freedom. This will not be the case here but MSM will be used to model the behavior of this system close to the bifurcation point.

The contribution starts with the short summary of the model development. Then the MSM will be shortly introduced. The main part will be dedicated to the analysis of the dynamical system corresponding to the isometric behavior of the muscle fibre. Both Fung's and quadratic form of the free energy are discussed.

2. Muscle fibre model based on GRT

In GRT the starting point is the initial configuration B_0 that "growths" and "remodels" , i.e. changes its volume ("growth"), anisotropy ("geometrical remodeling") or material parameters ("material remodeling"). This process is expressed at first by the tensor $\mathbf{P}$ (further growth

*Corresponding author. Tel.: +420 602 141 660, e-mail: rosen@kme.zcu.cz.

tensor) that relates the initial configuration to the relaxed one B_r with zero inner stress. To the real configuration B_t where the inner stress invoked by growth, geometrical remodeling and external loading can already exists, it is related by deformation tensor $\mathbf{F}_r$. According the work of DiCarlo [1] was in [3] developed the following system of equations describing the behavior of the muscle fibre

$$\mu = \frac{\partial\psi}{\partial c}; \quad \boldsymbol{\tau}_{el} = \frac{\partial\psi}{\partial \mathbf{F}}; \quad \boldsymbol{\tau}_{dis} = \mathbf{H}\dot{\mathbf{F}}; \quad \mathbf{GV} = \mathbf{C} - \mathbf{E}$$
$$\mathbf{M}\dot{\mathbf{K}} = \mathbf{R} - \frac{\partial\psi}{\partial \mathbf{K}}; \quad \mathbf{m} = -\mathbf{K_0}\mathbf{Grad}\mu \tag{1}$$

where $\psi(\mathbf{F}, \mathbf{K}, c)$ is the free energy related to the relaxed volume. $\mathbf{K}$ represents the material parameters, which can be changing during the material remodelling — $\dot{\mathbf{K}}$ is the corresponding velocity and $\mathbf{V} = \dot{\mathbf{P}}\mathbf{P}^{-1}$ is the velocity of growth. The stress $\boldsymbol{\tau}$ was decomposed into the elastic part $\boldsymbol{\tau}_{el}$ and the dissipative part τ_{dis}, $\mathbf{E}$ is the tensor of the Eshelby's type (further shortly Eshelby tensor), $\mathbf{M}, \boldsymbol{H}, \mathbf{K}_0$ and $\mathbf{G}$ are in the case of passive continua positively definite matrices. In [4] was shown, that in the application on muscle contraction this condition need not be fullfiled. The cause is the energy supply via ATP $\rightarrow$ ADP process. $\mathbf{C}$ is the generalized external remodelling force and μ and c are chemical potential and concentration of the relevant component respectively (see e.g. [4]). Here we will not deal with the physical interpretation of all these parameters but we apply the equations (1) on 1D continuum. Let's the 1D continuum has the initial length l_0. Its actual length after growth, remodeling and loading will be l. The relaxed length — it means after growth and remodeling — is l_r. For the corresponding deformation gradients we can write

$$P = \frac{l_r}{l_0}, \quad F = \frac{l}{l_r}, \quad \nabla p = \frac{l}{l_0}. \tag{2}$$

In the isometric case is $l = const$. For the free energy we will use the following form suggested by Fung:

$$\psi = \frac{k}{\mu}\left(e^{\frac{\mu}{2}(F-1)^2} - 1\right). \tag{3}$$

For $\mu \rightarrow 0$ we obtain the common form for linear elastic continuum

$$\psi = \frac{1}{2}k(F-1)^2 \tag{4}$$

and therefore the further obtained results will have more general meaning and can be interpreted also e.g. for the mentioned piezo-electric stack. Introducing from (2) and (3) into (1) we obtain the system of equations for the evolution of relaxed length (after growth), stiffness and stress (eventually force)

$$\dot{k} = \frac{1}{m}\left[r - \frac{1}{\mu}\left(e^{\frac{\mu}{2}(F-1)^2} - 1\right)\right],$$
$$\dot{l}_r = l_r^3 \frac{C + \frac{k}{\mu}e^{\frac{\mu}{2}(F-1)^2}\left[\mu\frac{l}{l_r}\left(\frac{l}{l_r} - 1\right) - 1\right] + \frac{k}{\mu}}{gl_r^2 + hl^2}, \tag{5}$$
$$\tau = k\left(\frac{l}{l_r} - 1\right)e^{\frac{\mu}{2}(F-1)^2} - hll_r\frac{C + \frac{k}{\mu}e^{\frac{\mu}{2}(F-1)^2}\left[\mu\frac{l}{l_r}\left(\frac{l}{l_r} - 1\right) - 1\right] + \frac{k}{\mu}}{gl_r^2 + hl^2}.$$

Here m, h and g correspond with the matrices $\mathbf{M}, \mathbf{H}$ and $\mathbf{G}$ in 1D case.

To be able to analyse the properties of the dynamical system we will rewrite the equations (5) into the dimensionless form. The values in these equations have the following dimensions:

τ, k, C .... [N]
l_r, l .... [m]
m .... [N^{-1}s]
g, h .... [Ns]
t .... [s]
r, μ .... [1]

We will introduce the following dimensionless variables

$$k' = k\sqrt{\frac{|m|}{g}}$$
$$l'_r = \frac{l_r}{l}$$
$$t' = \frac{t}{\sqrt{g|m|}}$$

Then we obtain the following equations:

$$\frac{dl'_r}{dt'} = {l'_r}^3 \frac{C + \frac{k'}{\mu}\sqrt{\frac{g}{|m|}} e^{\frac{\mu}{2}\left(\frac{1}{l'_r}-1\right)^2}\left[\mu\frac{1}{l'_r}\left(\frac{1}{l'_r}-1\right)-1\right] + \frac{k'}{\mu}\sqrt{\frac{g}{|m|}}}{\sqrt{\frac{g}{|m|}}{l'_r}^2 + h}, \tag{6}$$

$$\frac{dk'}{dt'} = \operatorname{sgn} m \left[r - \frac{1}{\mu}\left(e^{\frac{\mu}{2}\left(\frac{1}{l'_r}-1\right)^2} - 1\right)\right]. \tag{7}$$

Further simplification can be achieved introducing new variables

$$x = \frac{1}{l'_r}; \quad y = k'; \quad C' = C\sqrt{\frac{|m|}{g}}. \tag{8}$$

For $h = 0$ we obtain the equations of the autonomous dynamical system

$$\dot{x} = -x\left\{C' + \frac{y}{\mu}e^{\frac{\mu}{2}(x-1)^2}\left[\mu x(x-1) - 1\right] + \frac{y}{\mu}\right\}, \tag{9}$$

$$\dot{y} = \operatorname{sgn} m \left[r - \frac{1}{\mu}\left(e^{\frac{\mu}{2}(x-1)^2} - 1\right)\right]. \tag{10}$$

2.1. Analysis of stability

Now we try to analyse the properties of this system which depends only on four parameters C', r, μ and $\operatorname{sgn} m$. Further we will assume C' as a main control parameter. At first we find the coordinates of the equilibrium point

$$x_{eq} = \Theta + 1, \tag{11}$$

$$y_{eq} = -\frac{C'\mu}{(r\mu + 1)[\mu(\Theta + 1)\Theta - 1] + 1} \tag{12}$$

where

$$\Theta = \pm\sqrt{\frac{2}{\mu}\ln(r\mu+1)}. \tag{13}$$

Equations in variation for the system (9) and (10) are

$$\dot{\eta}_x = a_{11}\eta_x + a_{12}\eta_y \tag{14}$$
$$\dot{\eta}_y = a_{21}\eta_x + a_{22}\eta_y \tag{15}$$

where

$$\begin{aligned} a_{11} &= -y_{eq}(1+\Theta)^2(r\mu+1)(\Theta^2\mu+1) \\ a_{12} &= -\frac{1+\Theta}{\mu}\{(r\mu+1)[\mu(1+\Theta)\Theta-1]+1\} \\ a_{21} &= -\operatorname{sgn} m(r\mu+1)\Theta \\ a_{22} &= 0 \end{aligned} \tag{16}$$

Eigenvalues of the corresponding matrix are

$$\lambda_{1,2} = \frac{1}{2}\left[a_{11} \pm \sqrt{(a_{11})^2 + 4a_{12}a_{21}}\right]. \tag{17}$$

Assuming $a_{11} < 0$, $a_{12}a_{21} > 0$ the stability can be achieved e.g. for $\operatorname{sgn} m = -1$ and $C' < 0$. Detailed analysis will be done further for the simpler case $\mu \to 0$ — see Fig. 1. For $C' = 0 \Rightarrow y_{eq} = 0 \Rightarrow a_{11} = 0$ we have according to Grobman-Hartman theorem bifurcation (the equilibrium point is not hyperbolic — real part of the eigenvalue is zero). It can be shown that the conditions for the existence of the Hopf bifurcation usually cited (e.g. [8]) are fullfiled:

The first condition for the existence of Hopf's bifurcation

- zero RHS of the equations (9) and (10) for x_{eq}, y_{eq} given by equations (11) and (12) and $C' = 0$ is obviously satisfied.

- pure imaginary eigenvalues for $C' = 0$ exist if

$$-4a_{12}a_{21} > (a_{11})^2 \tag{18}$$

- condition of transversality for the real part of the eigenvalues has the form

$$\frac{\partial a_{11}}{\partial C} = \frac{\partial}{\partial C}\left[C\mu\frac{(1+\Theta)^2(r\mu+1)(\Theta^2\mu+1)}{(r\mu+1)[\mu(\Theta+1)\Theta-1]+1}\right] \neq 0 \tag{19}$$

and it is fulfiled for $\mu \neq 0, -\frac{1}{r}, -\frac{1}{\Theta^2}$. The experimental results did not confirm the existence of the non-degerated Hopf's bifurcation and therefore the deeper analysis is necessary. We will do it for the following two cases:

- At first we will analyse the above mentioned system with the Fung's formula ($\mu \neq 0$) using multiple scale method when the control parameter C' in the neighbourhood of zero is depending on ε^2 according to the recommendation in [8].

- Then we apply the limit procedure $\mu \to 0$ which corresponds to the quadratic form of the free energy and after detailed analysis of the stability conditions we use again the multiple scale method comparing the dependence of C' on ε^2 as in previous case and on ε.

2.2. Multiple-scale analysis — $\mu \neq 0$, $C' = \varepsilon^2 C_2$

We assume the following form of the solution

$$x = x_0 + \varepsilon x_1 + \varepsilon^2 x_2 + \varepsilon^3 x_3 \tag{20}$$

$$y = y_0 + \varepsilon y_1 + \varepsilon^2 y_2 + \varepsilon^3 y_3 \tag{21}$$

where $0 < \varepsilon \ll 1$ is the scalar parameter. All variables in (20) and (21) are function of T_0, T_1, T_2 where

$$T_0 = t, \quad T_1 = \varepsilon t, \quad T_2 = \varepsilon^2 t. \tag{22}$$

Before substituting from (20) and (21) into (9) and (10) we find the approximation for the exponential function

$$e^{\frac{\mu}{2}(x-1)^2} \cong e^{\frac{\mu}{2}(x_0-1)^2}\left[1 + \mu(x_0 - 1)(\varepsilon x_1 + \varepsilon^2 x_2 + \varepsilon^3 x_3)\right]. \tag{23}$$

Further we introduce the following expression for C'

$$C' = \varepsilon^2 C_2. \tag{24}$$

x_0 and y_0 are the fix point coordinates given in (11) and (12). For y_0 we can write

$$y_0 = \varepsilon^2 C_2 J \tag{25}$$

where

$$J = \frac{-\mu}{(r\mu + 1)[\mu(\Theta + 1)\Theta - 1] + 1} \tag{26}$$

Substituting now from (20) and (21) into (9) and (10) respecting the scaling of time (22) and neglecting the terms with exponent of ε greater then 3, we obtain

$$\begin{aligned}
&\frac{\partial x_0}{\partial T_0} + \varepsilon\frac{\partial x_0}{\partial T_1} + \varepsilon^2\frac{\partial x_0}{\partial T_2} + \varepsilon\frac{\partial x_1}{\partial T_0} + \varepsilon^2\frac{\partial x_1}{\partial T_1} + \varepsilon^3\frac{\partial x_1}{\partial T_2} + \varepsilon^2\frac{\partial x_2}{\partial T_0} + \varepsilon^3\frac{\partial x_2}{\partial T_1} + \varepsilon^3\frac{\partial x_3}{\partial T_0} = \\
&= -\varepsilon^2 x_0 \frac{C_2 J}{\mu}\left[e^{\frac{\mu}{2}(x_0-1)^2}\langle a_1\rangle + 1\right] - \varepsilon^3 x_0 C_2 J e^{\frac{\mu}{2}(x_0-1)^2}\langle a_2\rangle - \varepsilon x_0\left[\frac{y_1}{\mu}e^{\frac{\mu}{2}(x_0-1)^2}\langle a_1\rangle + \frac{y_1}{\mu}\right] - \\
&\quad - x_0\varepsilon^2\left[C_2 + y_1 e^{\frac{\mu}{2}(x_0-1)^2}\langle a_2\rangle + \frac{y_2}{\mu}e^{\frac{\mu}{2}(x_0-1)^2}\langle a_1\rangle + \frac{y_2}{\mu}\right] - \\
&\quad - x_0\varepsilon^3\left[y_1 e^{\frac{\mu}{2}(x_0-1)^2}\langle a_3\rangle + y_2 e^{\frac{\mu}{2}(x_0-1)^2}\langle a_2\rangle + \frac{y_3}{\mu}e^{\frac{\mu}{2}(x_0-1)^2}\langle a_1\rangle + \frac{y_3}{\mu}\right] - \\
&\quad - \varepsilon^3 x_1 \frac{C_2 J}{\mu}\left[e^{\frac{\mu}{2}(x_0-1)^2}\langle a_1\rangle + 1\right] - \varepsilon^2 x_1\left[\frac{y_1}{\mu}e^{\frac{\mu}{2}(x_0-1)^2}\langle a_1\rangle + \frac{y_1}{\mu}\right] - \\
&\quad - \varepsilon^3 x_1\left[C_2 + y_1 e^{\frac{\mu}{2}(x_0-1)^2}\langle a_2\rangle + \frac{y_2}{\mu}e^{\frac{\mu}{2}(x_0-1)^2}\langle a_1\rangle + \frac{y_2}{\mu}\right] - \varepsilon^3 x_2\left[\frac{y_1}{\mu}e^{\frac{\mu}{2}(x_0-1)^2}\langle a_1\rangle + \frac{y_1}{\mu}\right]
\end{aligned} \tag{27}$$

where

$$\langle a_1\rangle = \mu x_0^2 - \mu x_0 - 1 \tag{28}$$

$$\langle a_2\rangle = 2x_0x_1 - x_1 + (x_0 - 1)x_1(\mu x_0^2 - \mu x_0 - 1) \tag{29}$$

$$\langle a_3\rangle = 2x_0x_2 + x_1^2 - x_2 + \mu(x_0 - 1)x_1(2x_0x_1 - x_1) + (x_0 - 1)x_2(\mu x_0^2 - \mu x_0 - 1) \tag{30}$$

$$\begin{aligned}\langle a_4\rangle = {} & 2x_0x_3 - 2x_1x_2 - x_3 + \mu(x_0 - 1)x_1(2x_0x_2 + x_1^2 - x_2) + \\ & + \mu(x_0 - 1)x_2(2x_0x_1 - x_1) + (x_0 - 1)x_3(\mu x_0^2 - \mu x_0 - 1)\end{aligned} \tag{31}$$

and similarly for y

$$\frac{\partial y_0}{\partial T_0}+\varepsilon\frac{\partial y_0}{\partial T_1}+\varepsilon^2\frac{\partial y_0}{\partial T_2}+\varepsilon\frac{\partial y_1}{\partial T_0}+\varepsilon^2\frac{\partial y_1}{\partial T_1}+\varepsilon^3\frac{\partial y_1}{\partial T_2}+\varepsilon^2\frac{\partial y_2}{\partial T_0}+\varepsilon^3\frac{\partial y_2}{\partial T_1}+\varepsilon^3\frac{\partial y_3}{\partial T_0}= \\ =-\left[r-\frac{1}{\mu}\left(e^{\frac{\mu}{2}(x_0-1)^2}-1\right)\right]+ \\ +\varepsilon(x_0-1)x_1e^{\frac{\mu}{2}(x_0-1)^2}+\varepsilon^2(x_0-1)x_2e^{\frac{\mu}{2}(x_0-1)^2}+\varepsilon^3(x_0-1)x_3e^{\frac{\mu}{2}(x_0-1)^2} \tag{32}$$

Now we compare the members with the same exponent of ε. We obtain three following systems of equations (remember that x_0 and y_0 are constants!).

For ε^1:

$$\frac{\partial x_1}{\partial T_0}+y_1\frac{x_0}{\mu}\left[e^{\frac{\mu}{2}(x_0-1)^2}\langle a_1\rangle+1\right] = 0, \tag{33}$$

$$\frac{\partial y_1}{\partial T_0} = x_1(x_0-1)e^{\frac{\mu}{2}(x_0-1)^2}. \tag{34}$$

For ε^2:

$$\frac{\partial x_2}{\partial T_0}+y_2b_4 = -\frac{\partial x_1}{\partial T_1}-x_0C_2b_1-y_1x_1b_2+y_1x_1^2b_3, \tag{35}$$

$$\frac{\partial y_2}{\partial T_0}-x_2(x_0-1)e^{\frac{\mu}{2}(x_0-1)^2} = -\frac{\partial y_1}{\partial T_1}. \tag{36}$$

where

$$b_1 = \frac{J}{\mu}\left[e^{\frac{\mu}{2}(x_0-1)^2}\langle a_1\rangle+1\right]+1, \tag{37}$$

$$b_2 = x_0e^{\frac{\mu}{2}(x_0-1)^2}\left[2x_0-1+x_0(\mu x_0^2-\mu x_0-1)\right], \tag{38}$$

$$b_3 = x_0e^{\frac{\mu}{2}(x_0-1)^2}(\mu x_0^2-\mu x_0-1), \tag{39}$$

$$b_4 = \frac{x_0}{\mu}\left[e^{\frac{\mu}{2}(x_0-1)^2}\langle a_1\rangle-1\right]. \tag{40}$$

For ε^3:

$$\begin{aligned}\frac{\partial x_3}{\partial T_0}+\frac{\partial x_1}{\partial T_2}+\frac{\partial x_2}{\partial T_1} &= -x_0C_2Je^{\frac{\mu}{2}(x_0-1)^2}\langle a_2\rangle- \\ &-x_0\left[y_1e^{\frac{\mu}{2}(x_0-1)^2}\langle a_3\rangle+y_2e^{\frac{\mu}{2}(x_0-1)^2}\langle a_2\rangle+\frac{y_3}{\mu}e^{\frac{\mu}{2}(x_0-1)^2}\langle a_1\rangle+\frac{y_3}{\mu}\right]- \\ &-x_1\frac{C_2J}{\mu}\left[e^{\frac{\mu}{2}(x_0-1)^2}\langle a_1\rangle+1\right]- \\ &-x_1\left[y_1e^{\frac{\mu}{2}(x_0-1)^2}\langle a_2\rangle+\frac{y_2}{\mu}e^{\frac{\mu}{2}(x_0-1)^2}\langle a_1\rangle+\frac{y_2}{\mu}\right]- \\ &-x_2\left[\frac{y_1}{\mu}e^{\frac{\mu}{2}(x_0-1)^2}\langle a_1\rangle+\frac{y_1}{\mu}\right],\end{aligned} \tag{41}$$

$$\frac{\partial y_3}{\partial T_0}+\frac{\partial y_1}{\partial T_2}+\frac{\partial y_2}{\partial T_1} = (x_0-1)x_3e^{\frac{\mu}{2}(x_0-1)^2}. \tag{42}$$

From (33) and (34) we obtain the second order equation for x_1:

$$\frac{\partial^2 x_1}{\partial T_0^2} + \Omega^2 x_1 = 0 \tag{43}$$

where

$$\Omega^2 = (x_0 - 1)\frac{x_0}{\mu} e^{\frac{\mu}{2}(x_0-1)^2} \left[e^{\frac{\mu}{2}(x_0-1)^2} \langle a_1 \rangle + 1 \right]. \tag{44}$$

The solution is then

$$x_1 = K_1 \cos \Omega T_0 - K_2 \sin \Omega T_0 \tag{45}$$

$$y_1 = D(K_1 \sin \Omega T_0 + K_2 \cos \Omega T_0) \tag{46}$$

where $K_1(T_1, T_2)$, $K_2(T_1, T_2)$ and

$$D = \frac{\Omega}{\frac{x_0}{\mu} \left[e^{\frac{\mu}{2}(x_0-1)^2} \langle a_1 \rangle + 1 \right]}. \tag{47}$$

Now we will put this solution into (35) and (36). We can see, that the so called secular terms (terms containing $\sin \Omega T_0 \cos \Omega T_0$) are only the derivatives on the right sides of these equations (other terms contain products of x_1, y_1 and therefore goniometric functions with $2\Omega T_0$ and higher). The secular terms have to be zero and the sufficient condition for this is

$$\frac{\partial K_1}{\partial T_1} = \frac{\partial K_2}{\partial T_1} = 0 \Rightarrow K_1(T_2), K_2(T_2) \tag{48}$$

The solution of the remaining system of equations x_2, y_2 are the periodical function with the frequency $2\Omega T_0$. Next step would be inserting x_1, y_1 from (45) and (46) and x_2, y_2 into (41) and (42):

$$\frac{\partial x_3}{\partial T_0} + \frac{\partial x_1}{\partial T_2} = -x_0 C_2 J e^{\frac{\mu}{2}(x_0-1)^2} \langle a_2 \rangle - \\ - x_0 \frac{y_3}{\mu} \left[e^{\frac{\mu}{2}(x_0-1)^2} \langle a_1 \rangle + 1 \right] - x_1 \frac{C_2 J}{\mu} \left[e^{\frac{\mu}{2}(x_0-1)^2} \langle a_1 \rangle + 1 \right] - \tag{49}$$

– … terms with frequency 2Ω or higher

$$\frac{\partial y_3}{\partial T_0} + \frac{\partial y_1}{\partial T_2} = (x_0 - 1) x_3 e^{\frac{\mu}{2}(x_0-1)^2}.$$

The corresponding equation of the second order is

$$\begin{aligned} \frac{\mathrm{d}^2 x_3}{\mathrm{d}T_0^2} + \Omega^2 x_3 &= \frac{x_0}{\mu} \left[e^{\frac{\mu}{2}(x_0-1)^2} \langle a_1 \rangle + 1 \right] \frac{\partial y_1}{\partial T_2} - x_0 C_2 J e^{\frac{\mu}{2}(x_0-1)^2} \frac{\partial x_1}{\partial T_0} [2x_0 - 1 + (x_0 - 1)\langle a_1 \rangle] - \\ &- \frac{\partial x_1}{\partial T_0} \frac{C_2 J}{\mu} \left[e^{\frac{\mu}{2}(x_0-1)^2} \langle a_1 \rangle + 1 \right] - \frac{\partial^2 x_1}{\partial T_2 \partial T_0} \pm \ldots \end{aligned} \tag{50}$$

The secular terms on the RHS of (50) should be equal to zero. Inserting from (45) and (46) and comparing the coefficients by $\sin \Omega T_0$, $\cos \Omega T_0$ we obtain the equations for K_i

$$K_i' A + K_i B = 0 \tag{51}$$

where $K_i' = \partial K_i / \partial T_2$; $i = 1, 2$ and

$$\begin{aligned} A &= \Omega + D \frac{x_0}{\mu} \left[e^{\frac{\mu}{2}(x_0-1)^2} \langle a_1 \rangle + 1 \right], \\ B &= \Omega C_2 J \left\{ x_0 e^{\frac{\mu}{2}(x_0-1)^2} [2x_0 - 1 + (x_0 - 1)\langle a_1 \rangle] + \frac{1}{\mu} \left[e^{\frac{\mu}{2}(x_0-1)^2} \langle a_1 \rangle + 1 \right] \right\} \end{aligned} \tag{52}$$

(51) is the special form of the so called **reconstituted amplitude equations** [7] which is an asymptotic representation of a reduced dynamical system

$$\begin{bmatrix} \dot{K}_1 \\ \dot{K}_2 \end{bmatrix} = \dot{K} = G(K(\varepsilon), C(\varepsilon)). \tag{53}$$

The reconstituted amplitude equations allow generally to reduce the number of freedom to the codimension (that is the number of the pure imaginary and zero eigenvalues of (14), (15)). In this way this approach is equivalent to other reduction methods e.g. center manifold method. The condition (51) can be integrated and finally we obtain

$$K_i = K_{i0} e^{-\frac{B}{A} T_2}. \tag{54}$$

1. If the exponent is negative then K_i tend to zero and the equilibrium point is stable.
2. If the exponent is positive then K_i growth and the equilibrium point is unstable.
3. If the exponent is zero (e.g. for $C_2 = 0$) than the solution can be approximated by

$$x = x_0 + x_1 = x_0 + K_1 \cos \Omega T_0 - K_2 \sin \Omega T_0, \tag{55}$$
$$y = y_0 + y_1 = y_0 + D(K_1 \sin \Omega T_0 + K_2 \cos \Omega T_0). \tag{56}$$

This corresponds with the numerical experiments as will be shown further.

2.3. *Stability analysis for $\mu \to 0$*

Applying the limit procedure $\mu \to 0$ on (9) and (10) we obtain the equations

$$\dot{x} = -x \left[C' + \frac{y}{2} \left(x^2 - 1 \right) \right] \tag{57}$$
$$\dot{y} = \operatorname{sgn} m \left[r - \frac{1}{2} (x-1)^2 \right] \tag{58}$$

The equilibrium point has the coordinates

$$x_0 = 1 + \Theta, \quad y_0 = -\frac{2C'}{2\Theta + \Theta^2} \quad \text{where} \quad \Theta = \pm\sqrt{2r}. \tag{59}$$

Equations in variations have the form (14) and (15) where

$$a_{11} = 2C' \frac{(1+\Theta)^2}{\Theta(2+\Theta)}, \tag{60}$$
$$a_{12}a_{21} = \frac{1}{2} \operatorname{sgn} m \Theta^2 (1+\Theta)(2+\Theta). \tag{61}$$

Stability conditions $a_{11} < 0$, $a_{12}a_{21} < 0$ — see (17) — are fullfiled if

$$\begin{aligned} &\Theta > 0 \text{ and } \operatorname{sgn} m < 0 \text{ and } C' < 0; \\ &-1 < \Theta < 0 \text{ and } \operatorname{sgn} m < 0 \text{ and } C' > 0; \\ &-\infty < \Theta < -1 \text{ and } \operatorname{sgn} m < 0 \text{ and } C' < 0; \\ &-1 < \Theta < 0 \text{ and } \operatorname{sgn} m > 0 \text{ and } C' > 0; \end{aligned} \tag{62}$$

The situation in the parameter space is shown on Fig. 1. Non-hyperbolicity condition — that is zero real part of at least one of the eigenvalues (17) — is fullfiled for $a_{11} = 0 \wedge a_{12}a_{21} \leq 0$ or $a_{12}a_{21} = 0$ that is for $C' = 0$ or $\Theta = -1 \wedge \Theta = 0$ or $\Theta = -1$ or $\Theta = -2$. While the variables x_0, y_0 have to be positive, we will concentrate our attention on the neiboroghood of the point A for $\operatorname{sgn} m = -1$.

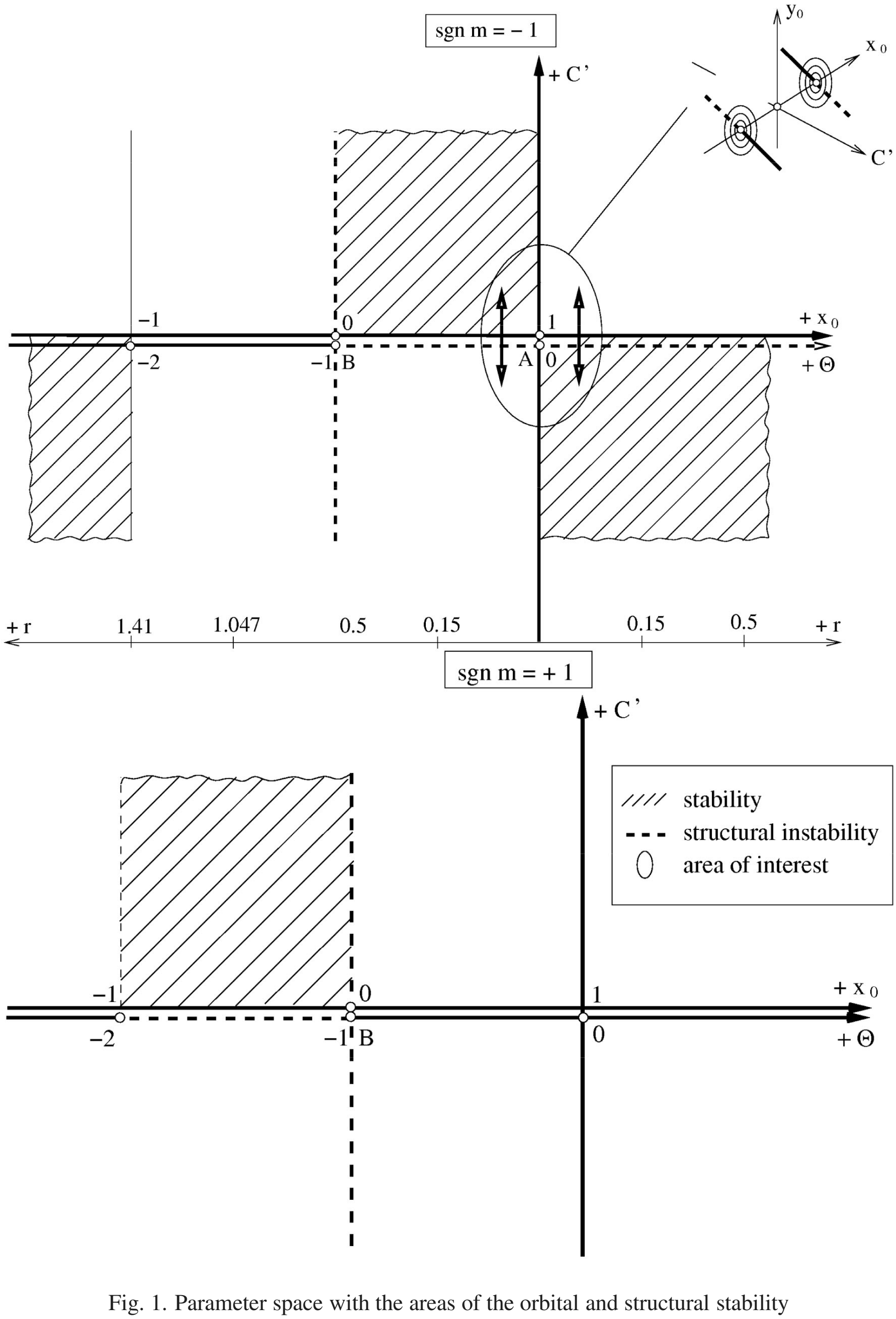

Fig. 1. Parameter space with the areas of the orbital and structural stability

2.4. Multiple-scale analysis for $\mu \to 0$, $C' = \varepsilon^2 C_2$

We apply the limit procedure $\mu \to 0$ on the above procedure and we obtain the **reconstituted amplitude equations** in form

$$2\Omega K_i' + \frac{1}{2}\frac{3\Theta^2 + 6\Theta + 2}{\Theta(\Theta+1) - r} K_i = 0 \tag{63}$$

which is the limit of (51). The discussion leads to the same consequences as above.

2.5. Multiple-scale analysis for $\mu \to 0$, $C' = \varepsilon C_1$

We try now to analyse the influence of the order of C' and insert $C' = \varepsilon C_1$. The corresponding equations are

$$\begin{aligned}
&\frac{\partial x_0}{\partial T_0} + \varepsilon\frac{\partial x_0}{\partial T_1} + \varepsilon^2\frac{\partial x_0}{\partial T_2} + \varepsilon\frac{\partial x_1}{\partial T_0} + \varepsilon^2\frac{\partial x_1}{\partial T_1} + \varepsilon^3\frac{\partial x_1}{\partial T_2} + \varepsilon^2\frac{\partial x_2}{\partial T_0} + \varepsilon^3\frac{\partial x_2}{\partial T_1} + \varepsilon^3\frac{\partial x_3}{\partial T_0} = \\
&= -\varepsilon_0^x \frac{C_1 J}{\mu}\left[e^{\frac{\mu}{2}(x_0-1)^2}\langle a_1\rangle + 1\right] - \varepsilon^2 x_0 C_1 J e^{\frac{\mu}{2}(x_0-1)^2}\langle a_2\rangle - \\
&- \varepsilon x_0 C_1 - \varepsilon x_0\left[\frac{y_1}{\mu}e^{\frac{\mu}{2}(x_0-1)^2}\langle a_1\rangle + \frac{y_1}{\mu}\right] - \\
&- x_0\varepsilon^3 C_1 J e^{\frac{\mu}{2}(x_0-1)^2}\langle a_3\rangle - x_0\varepsilon^2\left[y_1 e^{\frac{\mu}{2}(x_0-1)^2}\langle a_2\rangle + \frac{y_2}{\mu}e^{\frac{\mu}{2}(x_0-1)^2}\langle a_1\rangle + \frac{y_2}{\mu}\right] - \\
&- x_0\varepsilon^3\left[y_1 e^{\frac{\mu}{2}(x_0-1)^2}\langle a_3\rangle + y_2 e^{\frac{\mu}{2}(x_0-1)^2}\langle a_2\rangle + \frac{y_3}{\mu}e^{\frac{\mu}{2}(x_0-1)^2}\langle a_1\rangle + \frac{y_3}{\mu}\right] - \\
&- \varepsilon^2 x_1 \frac{C_1 J}{\mu}\left[e^{\frac{\mu}{2}(x_0-1)^2}\langle a_1\rangle + 1\right] - \\
&- \varepsilon^2 x_1 C_1 - \varepsilon^2 x_1 C_1 J e^{\frac{\mu}{2}(x_0-1)^2}\langle a_2\rangle - \varepsilon^2 x_1\left[\frac{y_1}{\mu}e^{\frac{\mu}{2}(x_0-1)^2}\langle a_1\rangle + \frac{y_1}{\mu}\right] - \\
&- \varepsilon^3 x_1\left[y_1 e^{\frac{\mu}{2}(x_0-1)^2}\langle a_2\rangle + \frac{y_2}{\mu}e^{\frac{\mu}{2}(x_0-1)^2}\langle a_1\rangle + \frac{y_2}{\mu}\right] - \varepsilon^3 x_2\frac{C_1 J}{\mu}\left[e^{\frac{\mu}{2}(x_0-1)^2}\langle a_1\rangle + 1\right] - \\
&- \varepsilon^3 x_2 C_1 - \varepsilon^3 x_2\left[\frac{y_1}{\mu}e^{\frac{\mu}{2}(x_0-1)^2}\langle a_1\rangle + \frac{y_1}{\mu}\right]
\end{aligned} \tag{64}$$

Using the similar approach as in the previous case we obtain the reconstituted amplitude equation in form:

$$K_i'(1 + D\Omega) - C_1 K_i[\ldots] = 0; \quad [\ldots] = 2\frac{x_0(x_0-1)}{\Theta(\Theta+2)}. \tag{65}$$

Integrating equation (65) we obtain

$$K_i = K_{i0}\exp\left\{C_1\frac{[\ldots]}{1 + D\Omega}T_1\right\}. \tag{66}$$

We can see, that in this problem the result does not depend on the order of C'.

3. Numerical experiments

On the following figures we can observe the influence of C on the phase portrait in the neighbourhood of the bifurcation point $C = 0$.

Fig. 2b corresponds to the bifurcation point. The limit cycle on the figure corresponds to the equations (55) and (56).

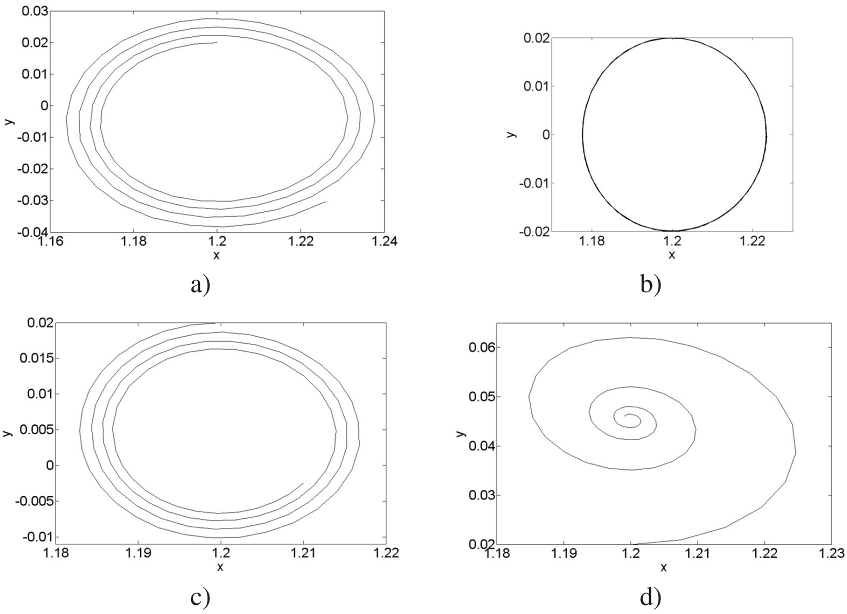

Fig. 2. Phase portrait for $C = \{0.001, 0, -0.001, -0.01\}$; starting point $x_0 = 1.2$, $y_0 = 0.02$, $\mu = 0.1$, $r = 0.02$

4. Conclusion

From the above demonstrated analysis we can extract conclusions:

1. In the presented cases the conditions (18), (19) do not justified the existence of the non-degenerated Hopf's bifurcation. This was proved via multiple-scale method and confirmed in numerical experiments. The reason is that also the fourth condition for the existence of this bifurcation has to be fulfilled: The bifurcation point should to be asymptotically stable — see e.g. [9]. We have shown that this is not the case.

2. The order of the approximation of the control parameter in this case did not influence the qualitative description of the system behaviour in the neiborough of the equilibrium points.

3. Both studied cases — with Fung's formula for the free energy potential and with the quadratic one — have the same qualitative properties.

4. The generalized external remodelling force influences essentially the phase portrait of the both dynamical systems. Especially interesting is the stable periodic motion for the zero value of this remodeling force.

5. On the other side it is necessary to stress that this phenomenon can be observed only if the change of stiffness is assumed!

Important task in future will be to try to find the real example of this periodic motion, e.g. in the muscle modeling where the external remodelling force corresponds to the outer control of the muscle contraction.

Acknowledgements

This paper has been supported by the project MSM 4977751303. The authors would like to express thanks to the anonymous reviewer for his very valuable comments and recommendations.

References

[1] A. DiCarlo, S. Quiligotti, Growth and balance. Mechanics Research Communications 29, PergamonPress, 2002, pp. 449–456.

[2] M. Forcinito, M. Epstein, W. Herzog, Can a rheological muscle model predict force depression/enhancement? Journal of Biomechanics 31 (1998) 1 093–1 099.

[3] J. Rosenberg, L. Hyncik, Contribution to the simulation of growth and remodelling applied to muscle fibre stimulation. In: Short communication of the 1st IMACS International Conference on Computational Biomechanice and Biology ICCBB 2007, Sept. 10–13, 2007, Plzeň, pp. 1–4.

[4] F. Maršík, I. Dvořák, Biothermodynamika. Academia, Praha, 1998.

[5] W. Herzog, Force enhancement following stretch af activated muscle: Critical review and proposal for mechanisms, Medical & Biological Engineering & Computing 2005, Vol. 43, 173–180.

[6] J. Rosenberg, L. Hyncik, Modelling of the piezo-effect based on the growth theory. In: Engineering Mechanics 2008, National Conference with international participation, May 12–15, 2008, Svratka, Czech republic.

[7] A. Luongo, A. Paolone, On the Reconstitution Problem in the Multiple Time-Scale Method, Nonlinear Dynamics 19, 1999, pp. 133–156.

[8] A. Nayfeh, B. Balachandran, Applied nonlinear dynamics. John Wiley, 1995.

[9] Jack H. Hale, Kocak, Hüseyin: Dynamics and Bifurcations. Springer-Verlag, New York, 1991.